3. J. J. Macklin, J. K. Trautman, T. D. Harris, L. E. Brus, *Science* **272**, 255 (1996).
4. D. A. Vanden Bout *et al.*, *Science* **277**, 1074 (1997).
5. W. E. Moerner, M. Orrit, *Science* **283**, 1670 (1999).
6. R. M. Dickson, A. B. Cubitt, R. Y. Tsien, W. E. Moerner, *Nature* **388**, 355 (1997).
7. X. S. Xie, *Acc. Chem. Res.* **29**, 598 (1996).
8. A. P. Bartko, R. M. Dickson, *J. Phys. Chem. B* **103**, 11237 (1999).
9. A. P. Marchetti, A. A. Muenter, R. C. Baetzold, R. T. McCleary, *J. Phys. Chem. B* **102**, 5287 (1998).
10. L. König, I. Rabin, W. Schulze, G. Ertl, *Science* **274**, 1353 (1996).
11. W. Harbich *et al.*, *J. Chem. Phys.* **93**, 8535 (1990).
12. S. Fedrigo, W. Harbich, J. Buttet, *J. Chem. Phys.* **99**, 5712 (1993).
13. C. Felix *et al.*, *Chem. Phys. Lett.* **313**, 105 (1999).
14. I. Rabin, W. Schulze, G. Ertl, *J. Chem. Phys.* **108**, 5137 (1998).
15. T. Tani, M. Murofushi, *J. Imaging Sci. Technol.* **98**, 1 (1994).
16. R. Kotz, E. Yeager, *J. Electroanal. Chem.* **111**, 105 (1980).
17. E. S. Brandt, *Appl. Spectrosc.* **47**, 85 (1993).
18. X. Q. Wang *et al.*, *Spectrochim. Acta A* **53**, 2495 (1997).
19. T. Watanabe, O. Kawanami, K. Honda, B. Pettinger, *Chem. Phys. Lett.* **102**, 565 (1983).
20. A. J. Varkey, A. F. Fort, *Sol. Energy Mater. Sol. Cells* **29**, 253 (1993).
21. T. Yamaguchi, S. Yoshida, A. Kinbara, *J. Opt. Soc. Am.* **64**, 1563 (1974).
22. H. P. Lu, L. Y. Xun, X. S. Xie, *Science* **282**, 1877 (1998).
23. H. Libardi, H. P. Grieneisen, *Thin Solid Films* **333**, 82 (1998).
24. B. Ohtani, S.-W. Zhang, T. Ogita, S. Nishimoto, T. Kagiya, *J. Photochem. Photobiol. A* **71**, 195 (1993).
25. P. S. Bechthold, U. Kettler, H. R. Schober, W. Krasser, *Z. Phys. D* **3**, 263 (1986).
26. I. Rabin *et al.*, *Chem. Phys. Lett.* **320**, 59 (2000).

27. We acknowledge stimulating discussions with R. L. Whetten and experimental assistance from L. A. Lyon and Z. L. Wang, and we gratefully acknowledge partial support of this project by the Georgia Institute of Technology Molecular Design Institute, under prime contract N00014-95-1-1116 from the Office of Naval Research and by the NSF Research Experiences for Undergraduates Program.

29 August 2000; accepted 20 November 2000

Toward Separation and Purification of Olefins Using Dithiolene Complexes: An Electrochemical Approach

Kun Wang* and Edward I. Stiefel*

The complex $Ni[S_2C_2(CF_3)_2]_2$ reacts with light olefins, including ethylene and propylene, selectively and reversibly. The reaction is not poisoned by hydrogen gas, carbon monoxide, acetylene, or hydrogen sulfide, which are commonly present in olefin streams, presumably because olefin binding occurs through the sulfur ligand rather than the metal center. The reversible reaction of olefins with $Ni[S_2C_2(CN)_2]_2^n$ ($n = 0, -1, -2$) can be controlled electrochemically, where the oxidation state–dependent binding and release of olefins are fast on the electrochemical time scale. The observed tolerance to poisons and controllable electrochemical reactivity present an alternative approach to the separation of olefins from complex streams.

Olefins are the largest volume feedstock in the chemical and petrochemical industry, and are widely used in the production of polymers, acids, alcohols, esters, and ethers (*1*). The lightest olefin, ethylene, is the largest volume organic chemical (*2*). Generally, olefins are produced via steam or catalytic cracking (*3, 4*) and separated by cryogenic distillation. The latter process is energy-intensive and costly, and contributes ~75% of the total olefin production cost (*5*). The large volume of olefins produced and the required purity for most applications provide strong incentives for novel alternative separation approaches.

The use of chemically specific separation reagents driven by electrical energy is a potentially inexpensive and efficient approach for separation (*6*). Indeed, redox-active metal salts such as copper (*7, 8*) have been reported to react with olefins reversibly. However, these metal-based systems are poisoned by C_2H_2, CO, and H_2S. Sulfur-containing systems such as those reported by DuBois *et al.* (*9*) might be tolerant to H_2S and CO, but react with H_2 and C_2H_2.

We report a reversible and robust system for olefin separation based on metal 1,2-enedithiolate (dithiolene) complexes. Whereas early interest in dithiolene complexes focused on their unusual redox and optical properties (*10–13*), recent studies have ranged from bioinorganic chemistry to material science (*14–16*). Schrauzer *et al.* (*17*) reported that $M(S_2C_2Ph_2)_2$ (M = Ni, Pd, Pt; Ph = phenyl group) reacts with norbornadiene, and Wing *et al.* (*18, 19*) reported that $Ni[S_2C_2(CF_3)_2]_2$ (**1**) reacts with norbornadiene and 2,3-dimethyl-1,3-butadiene to form 1/1 olefin adducts, where the olefin binds to ligand S atoms rather than the metal. However, there are no reports of such reactions with light unstrained mono-olefins. We found that, under mild conditions, **1** reacts with simple, aliphatic olefins selectively and reversibly to form 1/1 adducts.

Upon reaction with olefins, the deep purple solution of **1** turns light yellow, and the intensity of the lowest energy band (744 nm) in the ultraviolet-visible (UV-vis) spectrum decreases. The band at 744 nm [molar extinction coefficient $\varepsilon = 1050$ (toluene)] has been assigned as the transition between the highest occupied molecular orbital and the lowest unoccupied molecular orbital (HOMO→LUMO transition). When the adduct can be isolated (such as for norbornene and norbornadiene), the 744-nm band is absent. With simple olefins, the bands at 744 and 570 nm decrease with time (but do not fully disappear), and a band at 420 nm simultaneously appears, with an isosbestic point at 442 nm (Fig. 1). Similar patterns are observed for ethylene, propylene, *cis*-2-butene, 1-hexene, and *trans*-3-hexene. Exposure to an Ar atmosphere completely restores **1**, indicating that the reactions are fully reversible.

Low concentrations of H_2, CO, C_2H_2, H_2O, and H_2S may be present in typical olefin streams (*1*). These components generally poison metal-based complexing agents. However, when a solution of **1** (1 mM) was treated individually with pure (1 atm = 101.3 kPa) H_2, CO, C_2H_2, or water-saturated toluene under conditions used for ethylene binding, no reaction was observed. Moreover, the reaction with ethylene is not affected when 8 mole percent (~10 weight percent) H_2S is present, which is a far higher concentration than that found in typical olefin streams (*20, 21*). Clearly, **1** is tolerant to poisons potentially present in olefin streams, which we attribute to olefin binding at sulfur rather than the metal (Scheme 1). This unusual mode of olefin binding has been unambiguously demonstrated by x-ray crystallography for the norbornadiene adduct (*18*).

Kinetic studies were carried out using UV-vis spectroscopy for the reactions of 1-hexene and *trans*-3-hexene with **1**. Under pseudo–first order conditions, the plot of $\ln(A - A_e)$ versus time gives a straight line over three half-lives, revealing the reaction to be first-order in **1**. Plotting the observed rate constant k_{obs} against olefin concentration gives a straight line, indicating that the reaction is also first-order in olefin (Fig. 2). Consistent with a bimolecular reaction (Scheme 1) implied by the second-order kinetics, the mass spectrum (field desorption) of a solution of **1** in neat 1-hexene clearly shows a 1/1 adduct.

For ethylene and propylene, comparative

Corporate Strategic Research, ExxonMobil Research and Engineering Company, Route 22 East, Clinton Township, Annandale, NJ 08801, USA.

*E-mail: kwang@erenj.com (K.W.); eistief@erenj.com (E.I.S.)

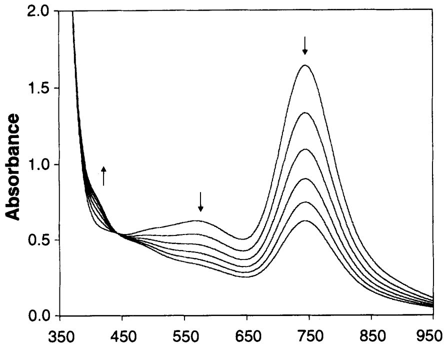

Fig. 1. Overlay of UV-vis spectra of **1** in the presence of C_2H_4 (in toluene at 30°C).

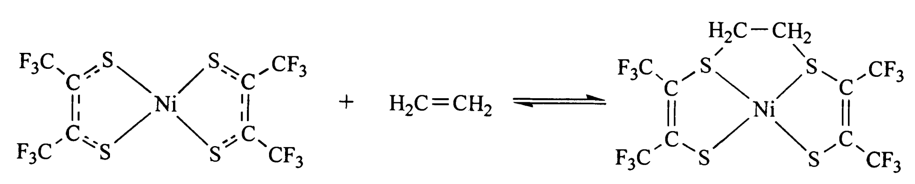

1

Scheme 1.

second-order reaction rates were estimated using the solubility of the olefin (*22, 23*). Kinetic and equilibrium results are listed in Table 1. The equilibrium constants for different olefins are roughly of the same magnitude, with bulkier olefins having somewhat smaller values. The reaction rates, however, are more sensitive to electronic aspects of the olefins. The faster reaction of propylene versus ethylene may be attributed to the more electron-rich double bond in propylene. Reactions with styrene and *p*-trifluoromethylstyrene (in toluene, 40°C) were examined to further probe the electronic effects. The initial rates are consistent with the trend that more electron-rich olefins react faster (styrene: $2 \times 10^{-3}\ M^{-1}\ s^{-1}$; *p*-trifluoromethylstyrene: $9 \times 10^{-4}\ M^{-1}\ s^{-1}$) (*24*), suggesting that **1** is electrophilic. The reaction can be viewed as electrophilic addition of **1** to the olefin, with the olefin donating electron density into the LUMO of **1**.

Temperature dependence kinetic studies reveal that the reaction with 1-hexene is mildly exothermic [enthalpy $\Delta H = -8.1(2)$ kcal/mol], suggesting that olefin binding is not very strong. The negative entropy of reaction [$\Delta S = -19(1)$ cal $mol^{-1}\ K^{-1}$ (or entropy units, e.u.)] is consistent with a bimolecular addition reaction. The activation parameters are: $\Delta H^{\ddagger} = 11(2)$ kcal/mol, $\Delta S^{\ddagger} = -36(5)$ e.u. (30° to 60°C). The large negative entropy of activation is consistent with the bimolecular addition reaction and indicates a highly ordered transition state. The activation parameters obtained here are consistent with those of Wing *et al.* for the reaction of **1** with norbornadiene ($\Delta H^{\ddagger} = 8.6$ kcal/mol, $\Delta S^{\ddagger} = -30$ e.u., in cyclohexane) (*25*).

Kinetic studies of the olefin binding reaction have been carried out in a range of solvents with different dielectric constants (ϵ). For 1-hexene, the rate is 6.7×10^{-4} ($M^{-1}\ s^{-1}$) in methylcyclohexane ($\epsilon = 2.02$), 1.1×10^{-3} in toluene ($\epsilon = 2.38$), and 7.7×10^{-3} in 1,2-dichloroethane ($\epsilon = 10.19$). The dramatic increase in rate with increasing solvent polarity (Table 1) suggests that charge separation occurs in the transition state, which is stabilized by polar solvents.

Most dithiolene compounds undergo multiple, reversible, one-electron redox reactions (*10*). Electrochemically oxidizing or reducing the complex should significantly affect its affinity for olefins and therefore offers a potential approach to manipulate olefin binding. This idea led us to explore the electrochemistry of this class of compounds in the presence of olefins.

For the electrochemical studies, we used $(Bu_4N)[Ni(mnt)_2]$, **2** [mnt = $S_2C_2(CN)_2^{2-}$; Bu = butyl group], which is well-behaved electrochemically, both alone and in the presence of olefins (Fig. 3). Although the neutral complex, $[Ni(mnt)_2]$, has never been isolated, it can be observed in rapid electrochemical reactions from either $[Ni(mnt)_2]^-$ or $[Ni(mnt)_2]^{2-}$ (**3**) (*12*). Neither **2** nor **3** reacts with olefins, as judged by the absence of reaction with norbornadiene (*26*). Cyclic voltammetry (CV) of **2** in CH_2Cl_2 shows two reversible couples (Fig. 3; $E_{1/2}$ = 0.69, −0.30 V versus ferrocene/ferrocenium couple, Fc/Fc^+), which have been assigned to the $Ni(mnt)_2/[Ni(mnt)_2]^-$ and $[Ni(mnt)_2]^-/[Ni(mnt)_2]^{2-}$ couples, respectively (*12*).

In the presence of excess 1-hexene, the $[Ni(mnt)_2]^-/[Ni(mnt)_2]^{2-}$ couple was virtually unaffected in the initial potential scan (Fig. 3). However, for the $[Ni(mnt)_2]/[Ni(mnt)_2]^-$ couple, the cathodic current i_c decreases significantly compared to the anodic current i_a (i_c/i_a = 0.43). This decrease suggests that $[Ni(mnt)_2]$, once formed, reacts promptly with 1-hexene, thereby reducing the concentration of "free" $[Ni(mnt)_2]$. There is no significant change in the i_c/i_a ratio when the scan rate is varied (100, 400, and 1000 mV/s), indicating that the reaction between $[Ni(mnt)_2]$ and 1-hexene is fast on the electrochemical time scale (on the order of seconds or subsecond). The nonzero value of i_c/i_a for the $[Ni(mnt)_2]/[Ni(mnt)_2]^-$ couple is consistent with an equilibrium reaction. Scanning to more negative potential {thereby

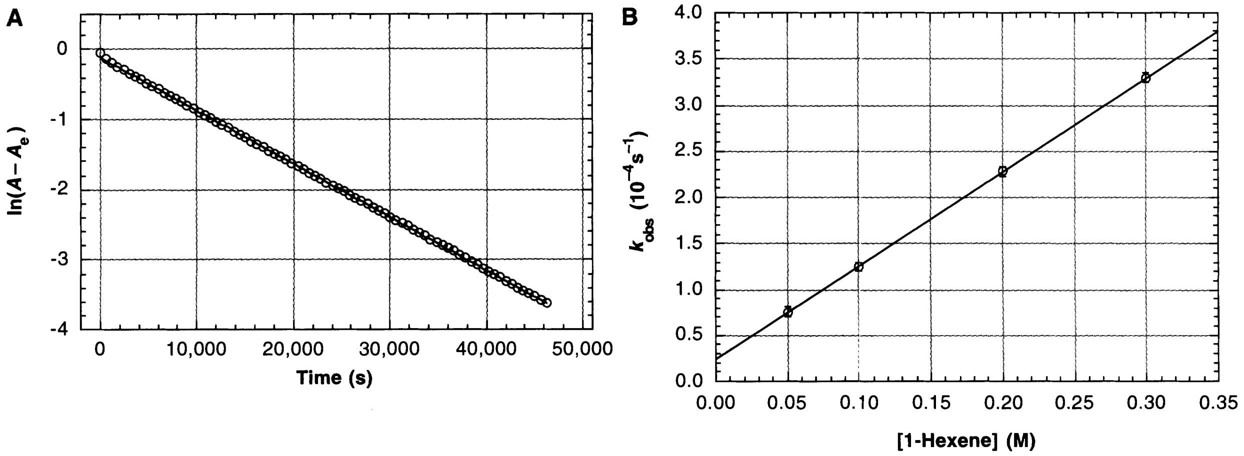

Fig. 2. Kinetics of the reaction of 1-hexene with **1** (in toluene at 30°C). (**A**) First-order plot (1 mM **1**, 0.05 M 1-hexene); (**B**) Second-order plot. The fitted line does not pass through the origin and should not for a reversible reaction. The intercept at k_{obs} is the rate constant for the reverse reaction (*30*).

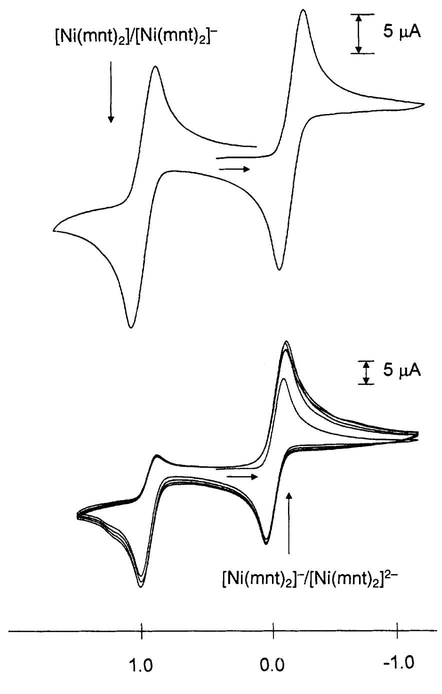

Fig. 3. Cyclic voltammagrams of **2** with no olefin present (top curve) and with 1-hexene (0.1 M) (bottom curve). Experimental conditions: 1 mM of **2** in CH_2Cl_2, 0.1 M Bu_4NPF_6 supporting electrolyte, Ag/Ag^+ reference electrode, scan rate = 100 mV/s. Potential reported in text is referenced to Fc/Fc^+ (0.23 V versus Ag/Ag^+).

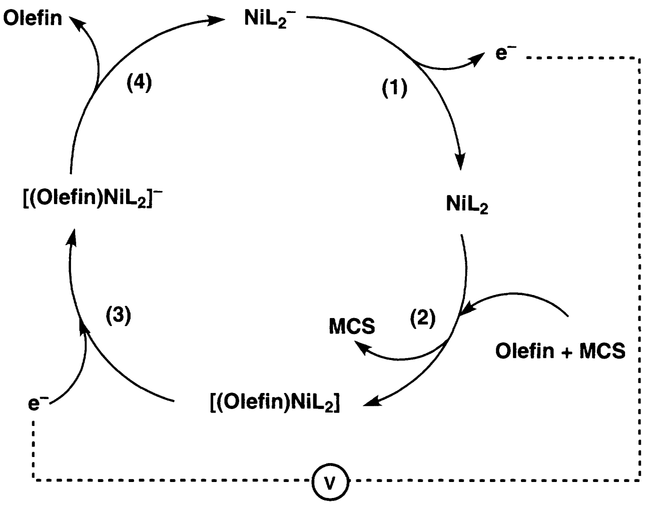

Fig. 4. Scheme for electrochemically driven olefin separation using nickel dithiolene complexes. (1) The mono-anionic complex [NiL_2^-] (L, ligand) is oxidized electrochemically, forming the neutral species [NiL_2]. (2) A multicomponent stream (MCS) containing an olefin(s) is introduced whereupon the olefin reacts with [NiL_2], forming the adduct [(olefin)NiL_2], while other (gaseous) components (such as alkanes, CO, C_2H_2, and so forth) pass unreacted. (3) The olefin adduct is electrochemically reduced. (4) The reduced olefin adduct [(olefin)NiL_2^-] releases olefin (which is recovered) as [NiL_2^-] is regenerated, completing the cycle. A similar scheme involves electrochemical reduction of the neutral species [NiL_2] that is in equilibrium with the olefin adduct [(olefin)NiL_2], which drives the release of the olefin from the adduct as the complexation equilibrium (Scheme 1) shifts to replenish the neutral species.

Table 1. Rate and equilibrium constants for reactions between olefins and $Ni[S_2C_2(CF_3)_2]_2$ at 30°C in toluene and 1,2-dichloroethane. ND, not determined.

Olefin	K_{eq} (M^{-1}) Toluene	k (10^{-4} $M^{-1}s^{-1}$)	
		Toluene	1,2-Dichloroethane
Ethylene	140	9	51
Propylene	70	25	153
1-Hexene	60	11	77
trans-3-Hexene	15	2	ND

reducing the 1-hexene adduct and/or the neutral [$Ni(mnt)_2$] species that is in equilibrium with the adduct} reveals that the $[Ni(mnt)_2]^-/[Ni(mnt)_2]^{2-}$ couple is only slightly broadened. However, the couple remains essentially reversible, indicating that the adduct quickly releases 1-hexene when reduced. The slight broadening in the shape of the $[Ni(mnt)_2]^-/[Ni(mnt)_2]^{2-}$ couple on further scanning suggests that the olefin adduct may, coincidentally, have a reduction potential similar to that of $[Ni(mnt)_2]^-$ ($E_{1/2}$ = −0.30 V versus Fc/Fc^+ for $[Ni(mnt)_2]^-/[Ni(mnt)_2]^{2-}$). Analogous behavior has been observed for the norbornadiene adduct with **1** (*18*) and the norbornene adduct with ReS_4^- (*27*). Multiple scans and scanning at different rates did not reveal any significant changes in the shape of either wave, indicating that there is a fast, clean, equilibrium reaction between 1-hexene and [$Ni(mnt)_2$]. Similar CV patterns have been observed for **2** in the presence of ethylene and propylene.

Our results show that fast olefin binding and release can be achieved and modulated electrochemically. Assuming a 1/1 stoichiometry for the adduct (*28*), the equilibrium constants can be estimated: 1-hexene, 7(1); propylene, 6(1); ethylene, and 5(1) M^{-1} (*29*). The small equilibrium constants and the rapid electrochemical response are consistent with facile olefin binding and release.

On the basis of these results, we propose an electrochemically driven olefin separation and purification scheme (Fig. 4). This scheme makes use of the rapid binding of an olefin by the electrochemically generated neutral dithiolene species and the subsequent release of the olefin upon electrochemical reduction of the adduct. Rapid switching of the potential at a given electrode or spatial separation of the anode and cathode lead to, respectively, temporal or spatial separation of the olefin from other components in the stream. Other reaction conditions such as temperature, pressure, and reaction media may be varied to favor olefin binding and/or release during electrochemical separation. Moreover, the choice of metal, ligand, and oxidation state provides great flexibility within this class of compounds for tuning the reactivity with olefins. Reversible olefin complexation to dithiolene complexes thus offers a novel approach to olefin separation and purification.

References and Notes

1. K. M. Sundaram, M. M. Shreehan, E. F. Olszewski, *Kirk-Othmer Encyclopedia of Chemical Technology* (Wiley, New York, ed. 4, 1995), pp. 877–915.
2. *Chem. Eng. News* **77** (no. 26), 32 (1999).
3. High-selectivity ethylene formation by partial oxidation of ethane has recently been reported [A. S. Bodke, D. A. Olschki, L. D. Schmidt, E. Ranzi, *Science* **285**, 712 (1999)].
4. P. K. Ladwig, in *Handbook of Petroleum Refining Processes*, R. A. Meyers, Ed. (McGraw-Hill, New York, ed. 2, 1997), chap. 3.1.
5. For example, ethane-ethylene separation is carried out at about −25°C and 320 psig (pounds per square inch gauge) (2.2 MPa) in a column containing more than 100 trays [R. L. Grantom, D. J. Royer, in *Ullmann's Encyclopedia of Industrial Chemistry* (VCH, New York, ed. 5, 1987), pp. 45–93].
6. National Research Council, "Separation and Purification: Critical Needs and Opportunities" (National Academy Press, Washington, DC, 1987).
7. G. C. Blytas, in *Separation and Purification Technology*, N. N. Li, J. M. Calo, Eds. (Dekker, New York, 1992), pp. 19–57.
8. T. Suzuki, R. D. Nobel, C. A. Koval, *Inorg. Chem.* **36**, 136 (1997).
9. M. McKenna *et al.*, *J. Am. Chem. Soc.* **105**, 5329 (1983).
10. J. A. McCleverty, *Prog. Inorg. Chem.* **10**, 49 (1968).
11. E. Billig, R. Williams, I. Bernal, J. H. Waters, H. B. Gray, *Inorg. Chem.* **3**, 663 (1964).
12. A. Davison, N. Edelstein, R. H. Holm, A. H. Maki, *Inorg. Chem.* **2**, 1227 (1963).
13. D. C. Olson, V. P. Mayweg, G. N. Schrauzer, *J. Am. Chem. Soc.* **88**, 4876 (1966).
14. P. Cassoux, L. Valade, *Coord. Chem. Rev.* **110**, 115 (1991).
15. J. A. Zuleta, M. S. Burberry, R. Eisenberg, *Coord. Chem. Rev.* **97**, 47 (1990).
16. R. S. Pilato, E. I. Stiefel, in *Bioinorganic Catalysis*, J. Reedijk, E. Bouwman, Eds. (Dekker, New York, ed. 2, 1999), pp. 81–152.
17. G. N. Schrauzer, V. P. Mayweg, *J. Am. Chem. Soc.* **87**, 1483 (1965).

18. R. M. Wing, G. C. Tustin, W. H. Okamura, *J. Am. Chem. Soc.* **92**, 1935 (1970).
19. A. Herman, R. M. Wing, *J. Organomet. Chem.* **63**, 441 (1973).
20. For a typical naphtha cracker, the concentration of total acid gases (CO_2 + H_2S) in the olefin stream entering a cryogenic tower is less than 1 ppm [p. 896 of (*1*)].
21. Under 1 atm of pure H_2S, reaction with H_2S is at least one order of magnitude slower than reaction with C_2H_4 under the same conditions, assuming a pseudo–first order reaction.
22. J. A. Waters, G. A. Mortimer, H. E. Clements, *J. Chem. Eng. Data* **15**, 174 (1970).
23. B. I. Konobeev, V. V. Lyapin, *Khim. Prom-st.* **43**, 114 (1967).
24. The reactions are not as clean as that with simple olefins (secondary reactions seem to occur, as indicated by UV-vis spectroscopy). Nevertheless, the initial reaction rates can be estimated from the UV-vis spectra.
25. J. R. Baker, A. Hermann, R. M. Wing, *J. Am. Chem. Soc.* **93**, 6486 (1971).
26. No reaction was observed when treating a solution of either **2** or **3** in CH_2Cl_2 with 100 equivalents of norbornadiene at 50°C for 1 week.
27. J. T. Goodman, T. B. Rauchfuss, *J. Am. Chem. Soc.* **121**, 5017 (1999).
28. The stoichiometry of the adduct with simple olefins has not yet been unambiguously established in the electrochemical reaction. Although we favor the 1/1 stoichiometry for the adduct with [Ni(mnt)$_2$] in analogy with the results for **1**, we cannot unequivocally rule out a 2/1 stoichiometry. Field desorption mass spectrum of the product formed by bulk electrolysis of **2** in the presence of norbornadiene suggests that two molecules of norbornadiene bind to [Ni(mnt)$_2$]. However, the norbornadiene result is not necessarily representative of the reactions with simple olefins due to the highly reactive nature of [Ni(mnt)$_2$] and norbornadiene.
29. When a large excess of olefin is used, the equilibrium constant can be reduced to: $K_{eq} = (1 - x)/(xC_0)$, where $x = i_c/i_a$ for the 0/–1 couple from the CV, and C_0 is the concentration of the olefin.
30. J. W. Moore, R. G. Pearson, *Kinetics and Mechanism* (Wiley, New York, ed. 3, 1981), p. 304.

31. We thank B. Cook, M. Matturro, J. Robbins, R. Espino, I. Horvath, J. McConnachie, C. Beswick, C. McConnachie, M. Greaney, R. Hall, J. Ou, M. Smith, and G. Stuntz for helpful discussions.

7 September 2000; accepted 21 November 2000

Timing of Millennial-Scale Climate Change in Antarctica and Greenland During the Last Glacial Period

Thomas Blunier[1]* and Edward J. Brook[2]

A precise relative chronology for Greenland and West Antarctic paleotemperature is extended to 90,000 years ago, based on correlation of atmospheric methane records from the Greenland Ice Sheet Project 2 and Byrd ice cores. Over this period, the onset of seven major millennial-scale warmings in Antarctica preceded the onset of Greenland warmings by 1500 to 3000 years. In general, Antarctic temperatures increased gradually while Greenland temperatures were decreasing or constant, and the termination of Antarctic warming was apparently coincident with the onset of rapid warming in Greenland. This pattern provides further evidence for the operation of a "bipolar see-saw" in air temperatures and an oceanic teleconnection between the hemispheres on millennial time scales.

Ice core and marine sediment records from the North Atlantic region show that climate during the last glacial period oscillated rapidly between cold and warm states that lasted for several thousand years. Understanding the manifestation of these rapid changes in other parts of the world may help unravel the underlying climate dynamics and predict the likelihood of future rapid climate change. Developing this understanding requires precise relative chronologies of events recorded in paleoclimate records. Polar ice cores provide one way of developing such a chronology for high-latitude sites.

Because of the rapid mixing time of the atmosphere ($\sim$1 year between hemispheres), large-scale changes in the concentration of long-lived atmospheric gases are essentially globally synchronous. This synchroneity provides a tool for correlating ice core chronologies and thereby comparing the timing of climate and other environmental change, recorded by various proxies in the ice, between the hemispheres. The correlation is complicated by the fact that air is trapped in bubbles 50 to 100 m below the surface, creating an age offset between the trapped air and the surrounding ice (*1*). This age offset (referred to as Δage) must be corrected for when comparing the timing of climate events recorded in the ice by stable isotopes or other proxies. Here we compare the timing of climate events in the Greenland Ice Sheet Project 2 (GISP2) ice core (Summit, Greenland) with the Byrd ice core (Byrd Station, Antarctica), using atmospheric methane as a correlation tool.

Blunier *et al.* (*2*) used methane records from the Greenland Ice Core Project (GRIP), Byrd, and Vostok to compare the timing of millennial-scale events between 10 and 45 thousand years ago (ka). They showed that warming in Antarctica preceded, by several millennia, the onset of warming in Greenland for Dansgaard-Oeschger (D-O) events 8 and 12—interstadial events that occurred at 38 and 45 ka (GISP2 chronology). Previous work showed a similar relationship for the Antarctic cold reversal and the Younger Dryas, cold periods that punctuate the last deglaciation in Antarctica and Greenland (*3*), respectively. Here we extend the comparison to 90 ka using new methane data from the Byrd ice core and existing records from GRIP and GISP2. The study of Blunier *et al.* (*2*) was based on data from the GRIP ice core and the GRIP time scale. However, the GISP2 ice core provides the most detailed northern CH_4 record between 40 and 110 ka, and we base our study on those results (*4*) and the GISP2 time scale (*5*). We adopt the GISP2 ice age time scale of Meese *et al.* (*6*) and the Δage calculations of Schwander *et al.* (*7*). We estimate the uncertainty in Δage from the uncertainty of the input parameters as $\pm$100 years between 10 to 20 ka, increasing to $\pm$300 years during the glacial period.

As expected, the Byrd and GISP2 methane records show a high degree of similarity. For example, between 53 and 60 ka both cores faithfully record a sequence of four major methane oscillations lasting 1000 years (1 ky) or less. Differences in concentration between the records are due to the latitudinal distribution of methane sources and sinks [(*8*) and references therein].

To create a gas age time scale for Byrd, we synchronized the Byrd methane record with the Greenland methane records from GISP2 and GRIP (*9*). We used a Monte Carlo method to search for a maximal correlation between the CH_4 records (*1*). For the period from 10 to 50 ka, we transferred the results of Blunier *et al.* to the GISP2 ice age time scale by correlating the rapid variations in $\delta^{18}O_{ice}$, which are virtually identical between GRIP and GISP2. We then adopted the previous correlation of GRIP and Byrd methane (*2*) to put the Byrd methane record for this period on the GISP2 time scale. For the time period from 50 to 90 ka, we directly correlated the

---

[1]Department of Geosciences, Guyot Hall, Princeton University, Princeton, NJ 08544, USA; Climate and Environmental Physics, Physics Institute, University of Bern, Sidlerstrasse 5, CH-3012 Bern, Switzerland. [2]Department of Geology and Program in Environmental Science, Washington State University, 14204 Northeast Salmon Creek Avenue, Vancouver, WA 98686, USA.

*To whom correspondence should be addressed. E-mail: blunier@princeton.edu